Contact-induced spin polarization of monolayer hexagonal boron nitride on Ni(111)

Cite as: Appl. Phys. Lett. **104**, 051604 (2014); https://doi.org/10.1063/1.4863324
Submitted: 11 November 2013 . Accepted: 13 January 2014 . Published Online: 04 February 2014

Manabu Ohtomo, Yasushi Yamauchi, Alex A. Kuzubov, Natalya S. Eliseeva, Pavel V. Avramov, Shiro Entani, Yoshihiro Matsumoto, Hiroshi Naramoto, and Seiji Sakai

Contact-induced spin polarization of monolayer hexagonal boron nitride on Ni(111)

Manabu Ohtomo,[1] Yasushi Yamauchi,[2] Alex A. Kuzubov,[3,4] Natalya S. Eliseeva,[3,4] Pavel V. Avramov,[1,3,4] Shiro Entani,[1] Yoshihiro Matsumoto,[1] Hiroshi Naramoto,[1] and Seiji Sakai[1]

[1]*Advanced Science Research Center, Japan Atomic Energy, Agency 2-4 Shirakata-Shirane, Tokai, Naka, Ibaraki 319-1195, Japan*
[2]*National Institute for Materials Science, 1-2-1 Sengen, Tsukuba, Ibaraki 305-0047, Japan*
[3]*L.V. Kirensky Institute of Physics SB RAS, Academgorodok, Krasnoyarsk 660036, Russia*
[4]*Siberian Federal University, 79 Svobodniy av., Krasnoyarsk 660041, Russia*

(Received 11 November 2013; accepted 13 January 2014; published online 4 February 2014)

Hexagonal boron nitride (h-BN) is a promising barrier material for graphene spintronics. In this Letter, spin-polarized metastable de-excitation spectroscopy (SPMDS) is employed to study the spin-dependent electronic structure of monolayer h-BN/Ni(111). The extreme surface sensitivity of SPMDS enables us to elucidate a partial filling of the in-gap states of h-BN without any superposition of Ni 3*d* signals. The in-gap states are shown to have a considerable spin polarization parallel to the majority spin of Ni. The positive spin polarization is attributed to the π-*d* hybridization and the effective spin transfer to the nitrogen atoms at the h-BN/Ni(111) interface. © *2014 AIP Publishing LLC*. [http://dx.doi.org/10.1063/1.4863324]

Hexagonal boron nitride (h-BN) with the honeycomb structure analogous to graphene is now becoming the focus of attention as an insulating material for graphene electronics and spintronics.[1–3] It has been recently demonstrated that electrical spins can be injected into graphene by using monolayer (ML) h-BN as an ultra-thin tunneling barrier between graphene and a ferromagnetic metal (FM) electrode.[2] Theoretical studies have also pointed out that the h-BN-based barrier layers could yield high magnetoresistance ratio and low junction resistance necessary for the efficient operation of spin valves.[4,5] The elucidation of the spin-dependent electronic structure of h-BN at the interfaces with FMs is particularly important for the design of graphene spintronic devices with the h-BN barrier layers.

The interactions between h-BN and Ni(111) have been considered to be physical in nature.[6,7] However, Preobrajenski *et al.* demonstrated with the X-ray absorption spectroscopy that there are unoccupied in-gap states induced by the hybridization between the Ni 3*d* and h-BN π orbitals at the interface.[8] The direct observation of the spin-dependent electronic structure of ML h-BN on FM has been challenging because in the conventional spin-resolved photoemission spectroscopy (PES) with a probing depth larger than several atomic layers, the weak signals from h-BN with a single atomic layer thickness are buried in the strong signals from the magnetic metal substrate.

In the present study, we selectively detected the electronic structure and spin polarization of the ML h-BN on Ni(111) by employing spin-polarized metastable-atom de-excitation spectroscopy (SPMDS).[9] The probe of the SPMDS are metastable triplet helium atoms (He*) with low kinetic energy (<0.1 eV), which enable surface-sensitive detection of the spin-dependent electronic structure. The SPMDS measurements on ML h-BN/Ni(111) elucidate that the π-*d* hybridization induce partially occupied in-gap states in ML h-BN. The in-gap states are shown to have a considerable spin polarization parallel to the majority spin of Ni and distributed on the outer surface, which indicate a possible influence on the spin dependent transport in spin valves using h-BN as a barrier material.

The experiments were performed in an ultra-high vacuum chamber with a base pressure of 3.0×10^{-8} Pa. The sample of ML h-BN/Ni(111) was prepared by ultra-high vacuum chemical vapor deposition (UHV-CVD).[10] The substrate was a W(110) single crystal with an atomically flat surface, which was prepared by the standard procedure.[11] An epitaxial Ni(111) film with 10 nm thickness was deposited on the W(110) surface at ambient temperature followed by short annealing at 873 K. h-BN was grown by exposing the Ni(111) surface to the vapor of borazine ($B_3N_3H_6$) at the substrate temperature of 873 K. The surface crystallinity and chemical composition were analyzed *in-situ* using low energy electron diffraction (LEED) and Auger electron spectroscopy (AES), respectively.

The surface electronic structure and spin polarization were investigated *in-situ* by the SPMDS measurements.[12,13] The sample was pulse-magnetized in-plane along the [1$\bar{1}$0] easy axis of magnetization of the Ni(111) thin film, and the SPMDS spectra were measured in remanence. The magnetic saturation was confirmed by measuring the magneto-optical Kerr effect. The spin polarization of the triplet He* was performed by optical pumping with 1083 nm circularly polarized radiation under a weak magnetic field (~0.1 G) defining a quantization axis as described previously.[9] The effective spin polarization P_{eff} of the beam was 0.74. The triplet He* atoms were adiabatically aligned parallel to the sample magnetization, using another constant magnetic field (~0.1 G) of Helmholtz coil.[13] By changing the helicity of the pumping radiation, the spin state of the He* atoms was switched between magnetic sub-levels ($m_s = +1$ and -1), namely, parallel and anti-parallel to the sample magnetization. The SPMDS spectrum was obtained by measuring the energy

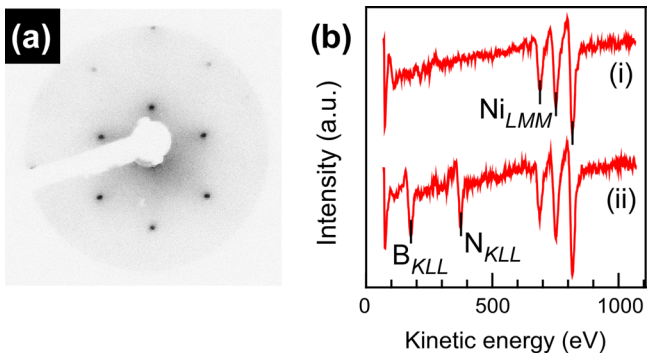

FIG. 1. (a) Low energy electron diffraction pattern of ML h-BN/Ni(111) after 100 L borazine exposure. The acceleration voltage was 275 V. (b) Auger electron spectra of (i) pristine Ni(111) and (ii) ML h-BN/Ni(111) after 100 L exposure. The electron energy was 3 keV.

spectrum of electrons emitted upon the de-excitation of He* atoms on the surface. The spin-dependent asymmetry of the SPMDS spectra, the spin asymmetry A, was defined as $A = \frac{1}{P_{eff}} \frac{I_{up} - I_{down}}{I_{up} + I_{down}}$, where I_{up} and I_{down} denote the secondary electron intensities under the irradiation of the He* beams spin-polarized parallel and anti-parallel to the sample magnetization direction, respectively.

The 1×1 growth of h-BN on Ni(111) was confirmed by LEED as shown in Fig. 1(a). The evolutions of the AES spectra (i) before and (ii) after borazine exposure are shown in Fig. 1(b). The peak intensity ratios of B *KLL* and N *KLL* to Ni *LMM* increased with borazine exposure and saturated at 100 L, because the h-BN growth is self-limited to a monolayer on Ni(111).[8,10,14]

Figs. 2(a) and 2(b) show the set of the SPMDS spectra measured with the spin-up and spin-down He* beams at different h-BN coverage θ, which are estimated from the peak intensity ratios in the AES spectra. With increasing the h-BN coverage, the broad spectrum with prominent feature at 10.5 eV observed for the pristine Ni(111) surface ($\theta = 0$) decreased in intensity and disappeared at $\theta = 1$. On the other hand, another feature appeared at 4.5 eV and increased in intensity with increasing θ. Moreover, the onset of the SPMDS spectrum shifts to the higher kinetic energy side, which indicates a reduction of the sample work function as discussed later.

The SPMDS spectra should be discussed with taking the de-excitation process of He* into account. As illustrated in Fig. 2(c), two processes can be involved in the He* de-excitation:[9,15] the resonance ionization (RI) + Auger neutralization (AN) process and the Auger de-excitation (AD) process. In the RI + AN process, which is dominant on the surface with a large density of unoccupied states around the Fermi level like metals, the He* atom is resonantly ionized above the surface by transferring the He* 2s electron to the unoccupied states of the sample via tunneling. The He ion is subsequently neutralized by filing the He* 1s hole with the valence electron of the sample, giving excess energy to another electron ejected from the surface. Since AN is the two-electron process, the RI + AN process gives rise to a broad and rather structureless SPMDS spectrum which reflects a self-convolution of the surface density of states (DOS). In contrast, the AD process is dominant on insulating surfaces, having a low density of unoccupied states and RI process is hampered. Instead, the He* atoms are de-excited by filling the 1s hole with the valence electron of the sample, which leads to the ejection of the 2s electron via the Auger process. Since AD process is one-electron process, the resultant spectrum is sharp with peaks directly comparable to density of states.

The dominant de-excitation process on ML h-BN/Ni(111) can be identified by measuring the evolution of the survival probability of the surface-scattered He* atoms. It is known that in the case of the RI + AN process, the efficient RI leads to the small survival probability of the He* atoms after the surface scattering as compared with the AD process.[16] Fig. 2(e) shows the exposure-dependent changes of the

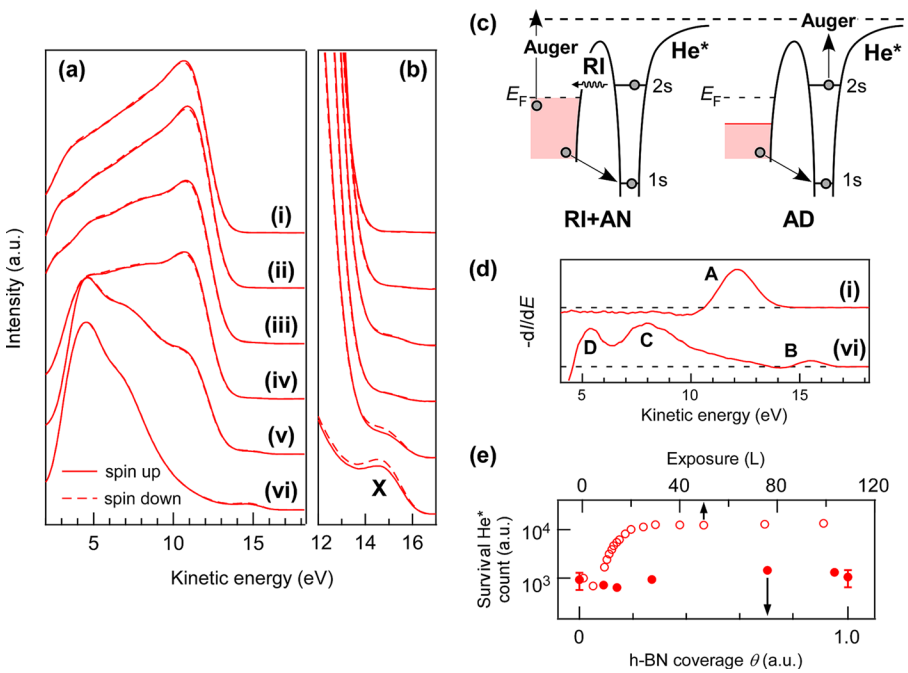

FIG. 2. (a) SPMDS spectra and (b) the enlargements for (i) pristine Ni(111) with a clean surface and (ii)–(vi) ML h-BN/Ni(111) at the h-BN coverage of (ii) $\theta = 0.09$ (1.2 L), (iii) $\theta = 0.14$ (2.4 L), (iv) $\theta = 0.27$ (5.4 L), (v) $\theta = 0.7$ (9 L), and (vi) $\theta = 1$ (100 L), respectively. The amounts of borazine exposure are denoted in the brackets. (c) Schematic diagram showing RI + AN (left panel) and AD (right panel) process of He*. (d) First derivatives of the SPMDS spectra (i) and (vi) in (a). (e) Intensities of the survival He* atoms after the surface scattering. The open and filled circles are for the multilayer benzene adsorption and for the ML h-BN growth on Ni(111), respectively. The counts are normalized by the He* beam flux.

intensities of the survival He* atoms, which are detected by the retarding energy analyzer with a high retarding potential shutting off electrons, during borazine exposure for the h-BN growth. The changes during benzene exposure for the multilayer benzene adsorption on Ni(111) at liquid nitrogen temperature are also shown for comparison. In the case of the benzene adsorption, the intensity increased by one order of magnitude with exposure. This is due to the change of the de-excitation process from RI + AN to AD with the growth of the insulating benzene multilayer on the metallic Ni(111). It is noteworthy that the survival He* intensity was not significantly affected by exposure in the case of the h-BN growth. This result indicates that the RI + AN process, which requires considerable density of unoccupied states around the Fermi level, is dominant on the ML h-BN surface contacted with Ni(111).

The maximum kinetic energy $E_{\mathrm{kin}}^{\mathrm{MAX}}$, which reflects the Fermi level of the sample, was 14.2 eV for the pristine Ni(111) surface ($\theta = 0$). As the h-BN coverage increased, the $E_{\mathrm{kin}}^{\mathrm{MAX}}$ shifted toward higher energies up to 16.6 eV at $\theta = 1$ (Fig. 2(b)). In the RI + AN process, $E_{\mathrm{kin}}^{\mathrm{MAX}}$ is expressed as[15]

$$E_{\mathrm{kin}}^{\mathrm{MAX}} = E_{\mathrm{I}} - \Delta E_{\mathrm{I}} - \varphi - \varphi_{\mathrm{A}},$$

where E_{I}, ΔE_{I}, φ, and φ_{A} are the ionization energy of the He atom (24.6 eV), the energy shift of the He* valence orbital approaching the surface due to electron-electron repulsion or image force potential,[17] the sample work function, and the analyzer work function, respectively. The shift of $E_{\mathrm{kin}}^{\mathrm{MAX}}$ as large as 2.4 eV can be ascribed to the reduction of φ and ΔE_{I}. The work functions of Ni(111) and ML h-BN ($\theta = 1$) on Ni(111) were estimated to be 5.1 eV and 3.6 eV, respectively, by ultra-violet photoemission spectroscopy. The remaining shift of 0.9 eV is due to the reduction of ΔE_{I} by lower electron density of h-BN cover layer than that of Ni, which is often observed on absorbate-covered surfaces.[18]

Since the SPMDS spectrum of 1 ML h-BN/Ni(111) was mainly derived from RI + AN de-excitation process, which is basically the self-convolution of density of states, the first derivative of SPMDS spectra are shown in Fig. 2(d) in order to illustrate features inherent to deconvoluted spectra[18] and directly comparable to surface DOS. In Fig. 2(d), the peak A is reasonably assigned to Ni 3*d* band.[9,19] The complete disappearance of peak A at $\theta = 1$ guarantees the extreme surface sensitivity of SPMDS. The peaks C and D distributed from 4 eV to 13 eV in the kinetic energy are assigned to the σ and π bands of h-BN, considering the Fermi level (16.6 eV) and the angle-resolved PES study.[7] The appearance of the peak B (and the peak X in Fig. 2(b)) in the vicinity of the Fermi level clearly shows the formation of new electronic states (in-gap states) in the band gap of h-BN. This result, together with the fact that the RI + AN process is dominant on the ML h-BN/Ni(111), suggests that the in-gap states are partially occupied with a considerable density of unoccupied states around the Fermi level.

Fig. 3 shows the spin asymmetry *A* calculated from the SPMDS spectra of Fig. 2(a). For the pristine Ni(111) surface ($\theta = 0$), the asymmetry of 9% is obtained around the $E_{\mathrm{kin}}^{\mathrm{MAX}}$ (14.2 eV). Since only an electron with spins antiparallel to the 1*s* electron spin is allowed to fill the 1s hole of the He*

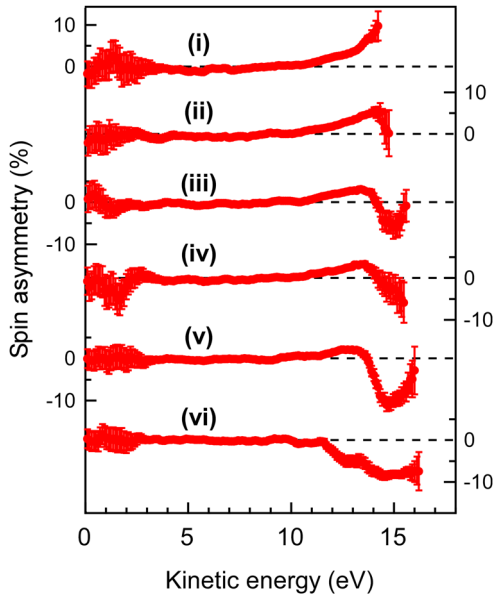

FIG. 3. Spin asymmetry derived from the sets of the SPMDS spectra (i)–(vi) of Fig. 2(a).

atom according to the Pauli exclusion principle, the positive spin asymmetry means a negative spin polarization of the surface electrons with respect to the majority spin of Ni. The h-BN growth on Ni(111) resulted in a significant change in the spin asymmetry, and a large negative asymmetry as large as $A = -8\%$ was observed at $\theta = 1$ in the region of the partially occupied in-gap states around the Fermi level (16.6 eV). The negative asymmetry indicates a positive spin polarization of the in-gap states. It is notable that the magnitude of the negative spin asymmetry was almost comparable to that of the positive asymmetry for the Ni(111) surface.

Density functional theory calculations provide insight into the nature of the electronic states and the spin polarization of ML h-BN on Ni(111). The calculational details are given in our previous report.[20] Figs. 4(a)–4(c) show the spin-resolved partial DOS (PDOS) of the B, N atoms, and the Ni atoms of ML h-BN/Ni(111) with the energetically favorable (N-*top*:B-*fcc*) configuration. In Figs. 4(a)–4(c), the ranges of the Ni 3*d* band (approximately from 5 to 0 eV) and the h-BN σ (from 12.3 to 4 eV) and π bands (from 10.3 to 4 eV) in the binding energy agree well with those of the peak A and the peaks C and D in the kinetic energy for Ni(111) and ML h-BN at $\theta = 1$ in Fig. 2(d). The hybridization between the antibonding π^* states and the Ni *d* states induces in-gap states of h-BN in the region from −3 eV to 3 eV of Figs. 4(a) and 4(b). The peak B in Fig. 2(d) and the corresponding peak X in Fig. 2(b) are reasonably attributed to the occupied in-gap states below the Fermi level. As can be seen from Fig. 4(b), the N p_z orbitals mainly contribute to the partially occupied in-gap states around the Fermi level. The results mentioned above clearly shows that the π-d hybridization at the interface makes the ML h-BN on Ni(111) metallic with a finite DOS at the Fermi level and consequently makes the RI + AN process dominant on the h-BN surface. It is notable that the in-gap states give rise to a large positive spin polarization just below the Fermi level, which is consistent with the large negative spin asymmetry observed in the SPMDS

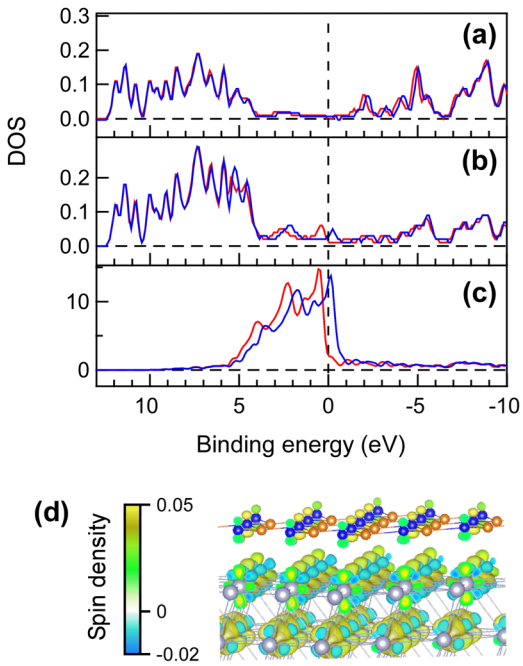

FIG. 4. (a) B, (b) N, and (c) Ni PDOS of ML h-BN/Ni(111). The blue and red solid lines represent the spin-up and spin-down PDOS, respectively. (d) Spatial distribution of the spin polarization from 1.2 eV to 0.1 eV in binding energy. The orange, blue, and gray spheres show B, N, and Ni atoms, respectively.

measurements. The π-d hybridization and the induced exchange splitting of h-BN together with the charge transfer mainly to the N p_z-derived orbitals reflecting the electronegativity of N lead to the effective spin transfer from the topmost Ni atoms to h-BN at the interface. As shown in Fig. 4(d), the in-gap states have a spin distribution on the outer surface as can be detected efficiently by SPMDS. It is plausible to assume that the spin-polarized in-gap states with spin densities distributed on the outer surface influence the sign and magnitude of the spin polarization of tunneling electrons in the magnetic tunnel junctions using h-BN as a barrier material.

In summary, the present SPMDS study has revealed that the ML h-BN on Ni(111) shows a metallic character, as judged from the RI + AN de-excitation process of the He* atoms, due to the in-gap states generated by the π-d hybridization at the interface. Moreover, the SPMDS spectra of h-BN exhibit a large negative spin asymmetry at around the Fermi level, which indicates a considerable positive spin polarization of the in-gap states in contrast to the negative polarization of Ni(111). The present study demonstrates that the application of h-BN could offer a promising way to optimize the operation of graphene-based spintronic devices.

This study was supported by the Grant-in-Aid for Scientific Research (Grant Nos. 23860067 and 24760033) from the Japan Society for the Promotion of Science.

[1]C. R. Dean, A. F. Young, I. Meric, C. Lee, L. Wang, S. Sorgenfrei, K. Watanabe, T. Taniguchi, P. Kim, K. L. Shepard, and J. Hone, Nat. Nanotechnol. **5**(10), 722 (2010).
[2]T. Yamaguchi, Y. Inoue, S. Masubuchi, S. Morikawa, M. Onuki, K. Watanabe, T. Taniguchi, R. Moriya, and T. Machida, Appl. Phys. Express **6**, 073001 (2013).
[3]S. Masubuchi, K. Iguchi, T. Yamaguchi, M. Onuki, M. Arai, K. Watanabe, T. Taniguchi, and T. Machida, Phys. Rev. Lett. **109**(3), 036601 (2012).
[4]O. V. Yazyev and A. Pasquarello, Phys. Rev. B **80**(3), 035408 (2009).
[5]V. M. Karpan, P. A. Khomyakov, G. Giovannetti, A. A. Starikov, and P. J. Kelly, Phys. Rev. B **84**(15), 153406 (2011).
[6]C. Oshima and A. Nagashima, J. Phys.: Condens. Matter **9**, 1 (1997).
[7]G. Grad, P. Blaha, K. Schwarz, W. Auwärter, and T. Greber, Phys. Rev. B **68**(8), 085404 (2003).
[8]A. Preobrajenski, A. Vinogradov, and N. Mårtensson, Phys. Rev. B **70**(16), 165404 (2004).
[9]M. Onellion, M. W. Hart, F. B. Dunning, and G. K. Walters, Phys. Rev. Lett. **52**(5), 380 (1984).
[10]A. Nagashima, N. Tejima, Y. Gamou, T. Kawai, and C. Oshima, Phys. Rev. Lett. **75**(21), 3918 (1995).
[11]R. Cortenraad, S. N. Ermolov, V. N. Semenov, A. W. D. van der Gon, V. G. Glebovsky, S. I. Bozhko, and H. H. Brongersma, J. Cryst. Growth **222**(1–2), 154 (2001).
[12]Y. Yamauchi and M. Kurahashi, Appl. Surf. Sci. **169**, 236 (2001).
[13]M. Kurahashi, T. Suzuki, X. Ju, and Y. Yamauchi, Phys. Rev. B **67**(2), 024407 (2003).
[14]W. Auwarter, T. J. Kreutz, T. Greber, and J. Osterwalder, Surf. Sci. **429**(1–3), 229 (1999).
[15]M. Kurahashi and Y. Yamauchi, Surf. Sci. **420**(2–3), 259 (1999).
[16]P. Fouquet and G. Witte, Phys. Rev. Lett. **83**(2), 360 (1999).
[17]H. D. Hagstrum, P. Petrie, and E. E. Chaban, Phys. Rev. B **38**(15), 10264 (1988).
[18]W. Sesselmann, B. Woratschek, J. Küppers, G. Ertl, and H. Haberland, Phys. Rev. B **35**(4), 1547 (1987).
[19]S. Entani, M. Kurahashi, X. Sun, and Y. Yamauchi, Carbon **61**, 134 (2013).
[20]P. V. Avramov, A. A. Kuzubov, S. Sakai, M. Ohtomo, S. Entani, Y. Matsumoto, H. Naramoto, and N. S. Eleseeva, J. Appl. Phys. **112**(11), 114303 (2012).